

1 **An optimisation strategy for evaluating modified Cam clay**  
2 **parameters using self-boring pressuremeter test data**

3 **Accepted for publication in Canadian Geotechnical Journal on 04/10/2018**

4  
5 **F.M. Gaone**

6 *Centre for Offshore Foundation Systems, University of Western Australia, Perth, Western*  
7 *Australia, Australia*

8 **J. P. Doherty**

9 *School of Civil, Environmental and Mining Engineering, University of Western Australia,*  
10 *Perth, Western Australia, Australia*

11 **S. Gourvenec**

12 *Faculty of Engineering and the Environment, University of Southampton, UK*

13

14 **ABSTRACT**

15 This paper presents an efficient, practical and automated strategy for deriving Modified Cam Clay  
16 parameters from undrained self-boring pressuremeter (SBPM) data. A mixed approach involving a  
17 parametric sweep and numerical optimisation is used, with a focus on parameter groups that dominate  
18 the Modified Cam Clay response in undrained cavity expansion. The proposed technique is illustrated  
19 using data from SBPM tests carried out in soft estuarine clay. The resulting parameters are used to back  
20 analyse large scale foundation load tests and are shown to provide an excellent match to the measured  
21 foundation response.

22 **INTRODUCTION**

23 Accurate prediction of foundation settlement is increasingly important in onshore and offshore  
24 geotechnical design. Onshore, reducing land space requires construction on non-ideal soils or above  
25 buried infrastructure while offshore, foundation footprints must be minimised to facilitate installation  
26 while ensuring tolerances on attached quasi-rigid infrastructure, such as pipelines and spools, are not  
27 compromised.

28 Despite advances in testing and modelling techniques, there is considerable evidence to show that there  
29 has been little genuine improvement in our ability to forecast foundation settlement over the past few  
30 decades. For example, in a recent international foundation prediction exercise, engineers were provided  
31 with extensive high quality laboratory and in situ test data and asked to forecast the undrained load-  
32 settlement response of a shallow foundation on soft clay to failure [1]. Fifty predictions were submitted  
33 from groups of engineers working in both industry and academia from 13 countries. The average  
34 predicted settlement under a load of 50% of the total bearing capacity exceeded the measured settlement  
35 by more than 1000%. For the 1.8 m square foundation, settlement predictions ranged from 0.1 mm to  
36 over 1200 mm, i.e more than 4 orders of magnitude. Similar findings have previously been presented  
37 for prediction exercises involving shallow foundations on soft clayey silt [2] and for the drained  
38 response of shallow foundations on sand [3,4]. A key reason for the huge variation in predictions is  
39 attributed to the fact that deriving parameters from test data requires considerable engineering/personal  
40 judgement. Removing subjectivity in parameter selection must therefore be regarded as critical in  
41 improving prediction performance. To do this, automated parameter selection techniques are required,  
42 in which test data are the input and engineering parameters are the output. This paper presents such a  
43 technique where undrained pressuremeter data is the input and Modified Cam Clay parameters are the  
44 output.

45 Self-boring pressuremeter (SBPM) testing enables in situ non-linear stress-strain response to be  
46 captured at different stress levels (depths) over a large range of strain, with minimal soil disturbance.

47 The SBPM is an advancement of the 1955 patented Ménard pressuremeter, developed in the 1970s to  
48 reduce soil disturbance caused by pre-drilling the borehole. Existing interpretation methods allow the  
49 derivation of in situ horizontal stress, stiffness parameters and undrained shear strength from  
50 pressuremeter data. These values may be used as parameters for elastic perfectly-plastic constitutive  
51 models. However, these models are inherently limited in their ability to describe real soil behaviour.

52 Determining parameters for more advanced soil constitutive models, such as Modified Cam Clay  
53 (MCC), from SBPM data is complicated by the fact that the parameters that control the model response  
54 are not directly visible in the measured data. Therefore, numerical models that represent the boundary  
55 conditions of the field test must be created and constitutive model parameters systematically varied

56 until an optimal match between test data and model response is achieved. If done manually, this process  
57 can be complex, time consuming and it is difficult to ensure an optimal set of parameters has been  
58 identified. Attempts to derive constitutive model parameters from pressuremeter test data using  
59 numerical optimisation are reported in the literature [3,4], but these approaches require the use of  
60 additional information or resources to determine a complete parameter set.

61 Challenges are also reported in the literature for the simpler task of deriving MCC parameters from  
62 undrained triaxial compression tests using optimisation techniques [5–10]. This challenge has since  
63 been solved with a two-step single variable optimisation approach for normally consolidated triaxial  
64 data based on ‘composite’ MCC parameters [11]. This paper presents a similarly efficient and  
65 automated approach for identifying an optimal or near optimal set of Modified Cam Clay parameters  
66 from undrained self-boring pressuremeter test data. The concept of the two-step single variable  
67 numerical targeted optimisation approach was adopted in this study, yet the procedure developed is  
68 inherently different to that based on triaxial compression test data [11], since the data obtained from the  
69 SBPM tests used as the input into the optimisation process is inherently different to the data that is  
70 obtained from triaxial tests and therefore requires different strategies and constraints to determine an  
71 optimised parameter set.

72 Our objective is to derive a set of MCC parameters that can be used to forecast the undrained load-  
73 displacement response of a shallow foundation. This problem is dominated by the soil strength and the  
74 shear stiffness, and less so by the volumetric stiffness (that is measured in a one-dimensional or isotropic  
75 compression test). Therefore, the MCC model was calibrated against self-boring pressuremeter data,  
76 which is strongly influenced by strength and shear stiffness of the soil.

77 The strategy developed in this paper relies on using standard interpretation methods to derive the initial  
78 mean effective stress (from the lift off pressure) and the undrained shear strength from final slope of  
79 pressuremeter pressure-expansion curve. This information is then used to constrain the MCC  
80 parameters that link effective stress and undrained shear strength. This significantly limits the possible  
81 set of valid soil parameters and enables an organised search and single variable optimisation procedure  
82 to be established.

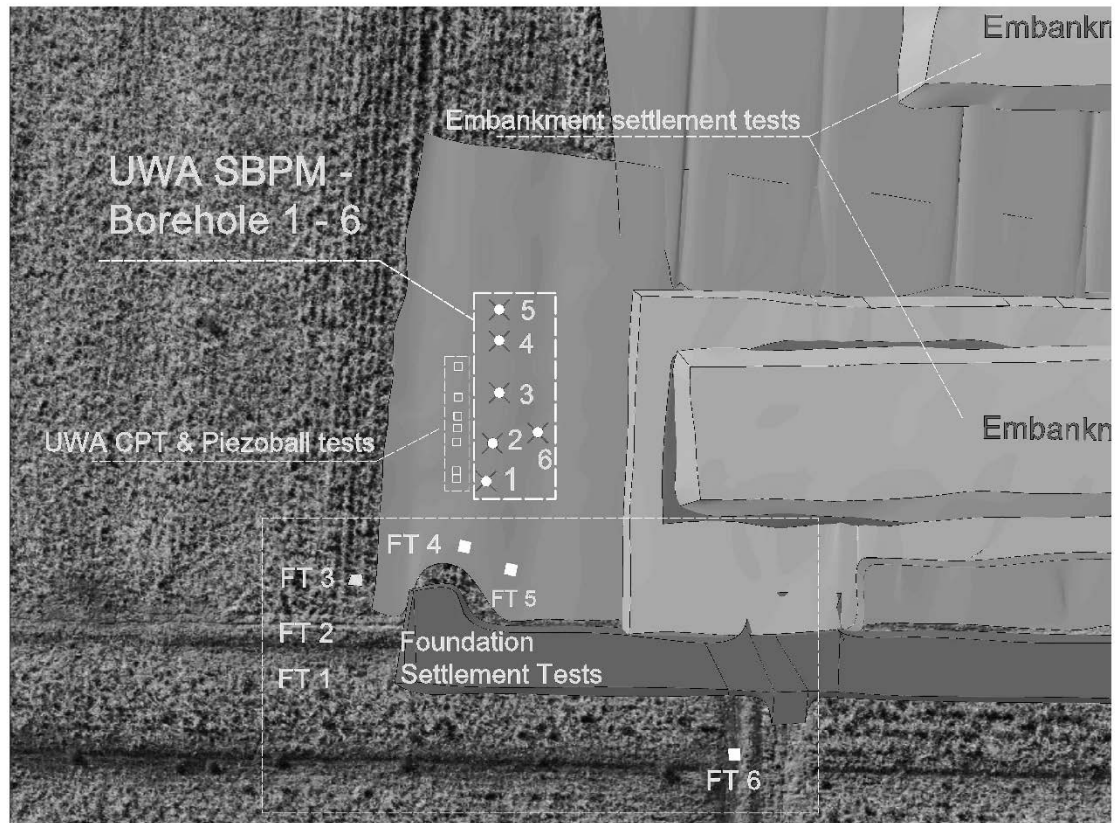
83 In the following sections, key aspects of the self-boring pressuremeter (SBPM) tests are presented along  
84 with the numerical model to represent the field tests; the Modified Cam Clay (MCC) model is set out,  
85 with particular emphasis on the composite parameter sets utilised in the approach developed in this  
86 study; the optimisation strategy for estimating an optimal (or near optimal) set of MCC parameters from  
87 the SBPM data is then described in detail; the strategy is applied to a set of SBPM results; and finally  
88 the strategy is validated by using the resulting optimised set of MCC parameters to back-analyse the  
89 load-settlement response of a shallow foundation field test.

90 The self-boring pressuremeter data used in this study, along with a range of other field and laboratory  
91 test data from the site and the results of the shallow foundation load-settlement tests have been made  
92 publically available in digital form at [www.geocalcs.com/datamap](http://www.geocalcs.com/datamap) [12].

### 93 **SELF-BORING PRESSUREMETER TESTING**

94 Self-boring pressuremeter (SBPM) testing was carried out in soft estuarine clay at the National Field  
95 Testing Facility (NFTF) in Ballina, New South Wales, Australia as part of a wider field testing  
96 programme [13]. Figure 1 shows an aerial image of the NFTF with the positions of the SBPM tests,  
97 along with the location of other in situ characterisation tests and shallow foundation and embankment  
98 field tests.

99 The full SBPM programme comprised 27 tests with the newly refurbished University of Western  
100 Australia (UWA) self-boring pressuremeter [14], carried out in six boreholes between 2 m and 9 m  
101 below ground level, with and without unload-reload loops, at different loading rates and with stress  
102 holding periods to assess consolidation and creep. In this paper, eight tests from three boreholes (2, 3  
103 and 4 in Figure 1) from depths between 2.00 m and 5.50 m are considered. These tests were selected as  
104 they did not involve unload/reload loops or stress holding periods and were carried out at a rate to ensure  
105 an undrained soil response. Details of and results from the entire programme of testing are presented in  
106 a separate publication [14]. The purpose of this paper is to set out and verify the targeted numerical  
107 optimisation strategy for determining an optimal or near optimal set of Modified Cam Clay parameters  
108 from SBPM tests for use in predicting the undrained load-settlement response of a shallow foundation.



109

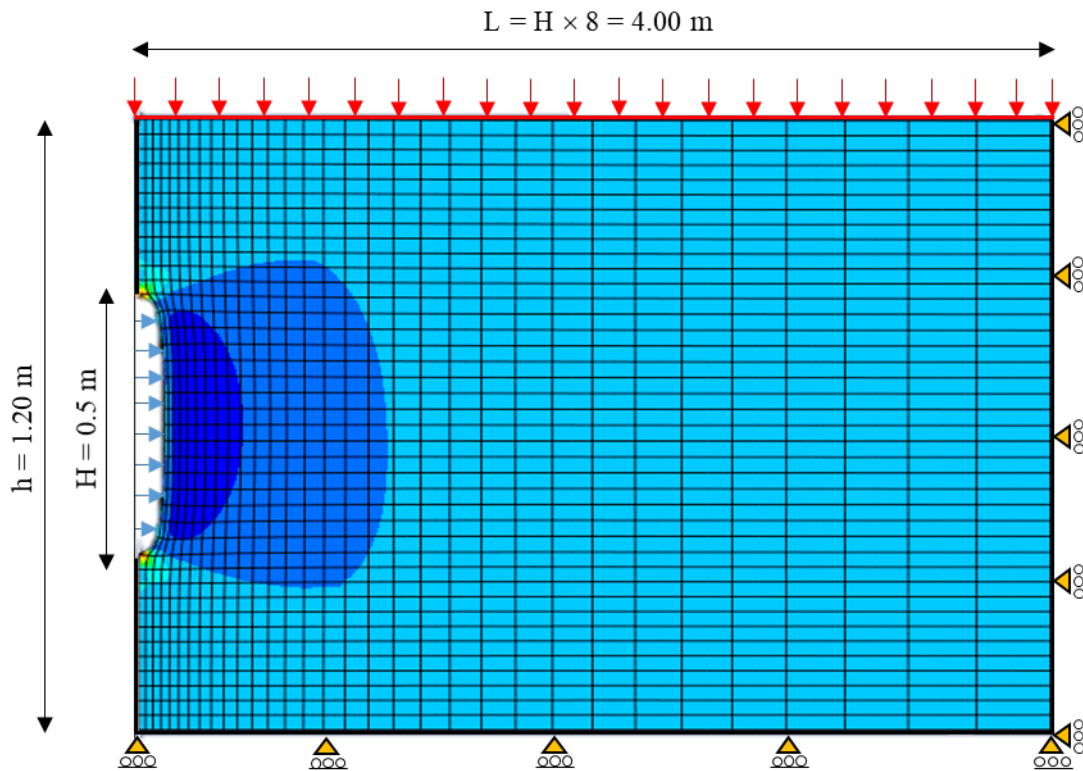
110 Figure 1: Aerial view of the NFTF showing the location of the SBPM tests, other in situ soil  
 111 characterisation tests and foundation and embankment settlement tests.

112

113 **NUMERICAL MODEL**

114 A two-dimensional axisymmetric finite element model was developed to simulate the field SBPM tests  
 115 in order to generate the numerical responses necessary to compare with field test data. The model was  
 116 created with the finite element software package, Abaqus [15], and comprised 1767 8-noded quadratic  
 117 elements (Figure 2). The pressuremeter cavity was modelled in a soil domain extending 0.7 times the  
 118 height of the pressuremeter above and below the cavity and 100 times the radius of the pressuremeter  
 119 in the radial direction. Displacements were constrained in the vertical direction across the base and in  
 120 the radial direction on the outer edge. A constant pressure boundary condition was applied to the upper  
 121 surface to represent the overburden pressure. A parametric study was conducted to ensure that the  
 122 boundaries were positioned to ensure the restraints did not influence the simulation results. The

123 expansion of the cavity wall was achieved by a prescribed radial pressure equal to the cavity pressure  
124 in the field tests. MATLAB and Python scripts were used to automate the variation of input parameters  
125 and post processing of output data. The soil was represented with the Modified Cam Clay model  
126 available in Abaqus (Clay Plasticity), described in the following section.  
127



128

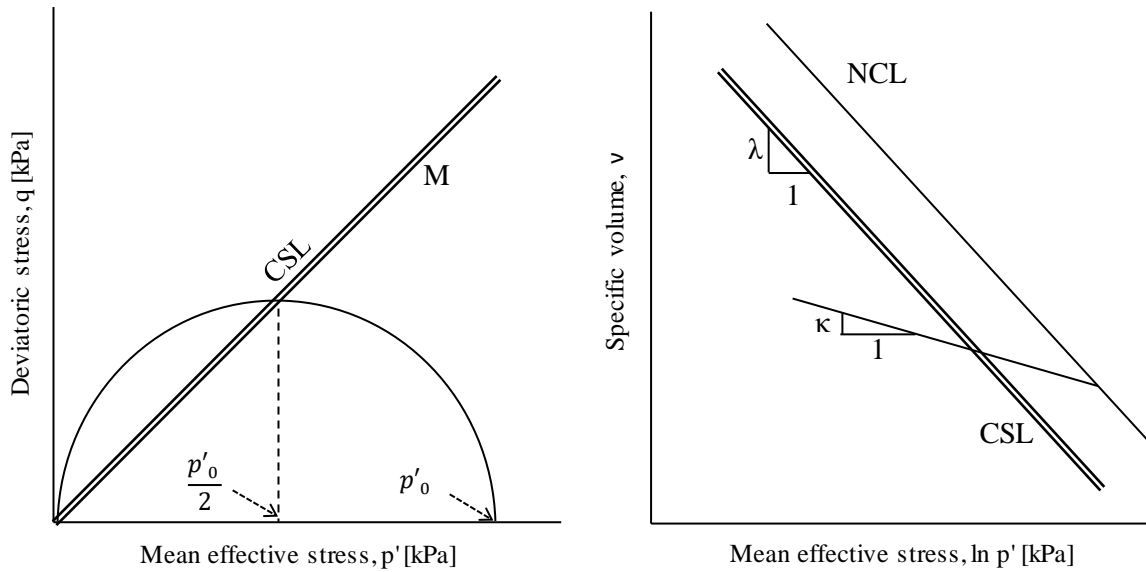
129

Figure 2: Finite element mesh for SBPM test simulation.

### 130 MODIFIED CAM CLAY MODEL & COMPOSITE PARAMETERS

131 The Modified Cam Clay (MCC) model [16] is based on critical state theory with a logarithmic  
132 relationship between the mean effective stress,  $p'$ , and the specific volume,  $v$  and an elliptical yield  
133 surface in mean effective stress,  $p'$ , deviatoric stress,  $q$ , space (Figure 3). The basic parameters of the  
134 Modified Cam Clay model are listed in Table 1.

135



136

137 Figure 3: Modified Cam Clay representation in  $p':q$  and  $v/\ln p'$  space. (CSL = Critical state line; NCL  
 138 = Normal compression line)

139 Table 1: Definition of Modified Cam Clay parameters

Parameter	Value
$\lambda$	Slope of the normal compression line (NCL)
$\kappa$	Slope of the unload reload line
$v$	Specific volume
$M$	Slope of the critical state line (CSL) in $p':q$ plane
$\mu$	Poisson's ratio

140

141 The stress state is defined under triaxial conditions by the mean effective stress,  $p'$ , and the deviatoric  
 142 stress,  $q$ , where

(1)	$p' = \frac{(\sigma'_1 + 2\sigma'_3)}{3}$
-----	---

143 and

(2)	$q = (\sigma'_1 - \sigma'_3)$
-----	-------------------------------

144 where  $\sigma'_1$  and  $\sigma'_3$  are the major and minor principal effective stresses respectively.

145 The elliptical yield surface in the  $p':q$  plane is defined by

(3)	$\frac{p'_0}{p'} = \frac{M^2 + \eta^2}{M^2}$
-----	--

146 where  $p'_0$  is the isotropic pre-consolidation pressure,  $M$  is the slope of the critical state line and

147  $\eta = q/p'$ . Inside the yield surface the model is elastic, with a shear modulus given by

(4)	$G = \frac{3(1 - 2\mu)\nu p'}{2(1 + \mu)\kappa} = \frac{3(1 - 2\mu)p'}{2(1 + \mu)\kappa^*}$
-----	---

148 The elastic shear stiffness can be expressed with a constant Poisson's ratio,  $\mu$ , and varying shear

149 modulus,  $G$ , or vice versa. In this study Poisson's ratio,  $\mu$  was kept constant while the shear modulus,

150  $G$ , varied with the mean effective stress,  $p'$ .

151

152 The undrained shear strength can be determined from MCC parameters as

(5)	$s_u = \frac{p'_i M}{2} \left( \frac{R_0}{2} \right)^\Lambda$
-----	---

153 Where the exponent  $\Lambda$  is given by

(6)	$\Lambda = \frac{\lambda - \kappa}{\lambda}$
-----	--

154  $R_0$ , is the isotropic overconsolidation ratio, given by the ratio of the maximum mean effective stress,

155  $p'_0$ , and the initial mean effective stress,  $p'_i$

(7)	$R_0 = \frac{p'_0}{p'_i}$
-----	---------------------------

156 In the MCC formulation, the two compression indices,  $\kappa$  and  $\lambda$ , always appear in combination with the

157 specific volume,  $v$ . For an undrained response, for which  $v$  is constant, this allows the number of MCC

158 parameters to be reduced by introducing the composite parameters



(8)	$\kappa^* = \frac{\kappa}{\nu}$
-----	---------------------------------

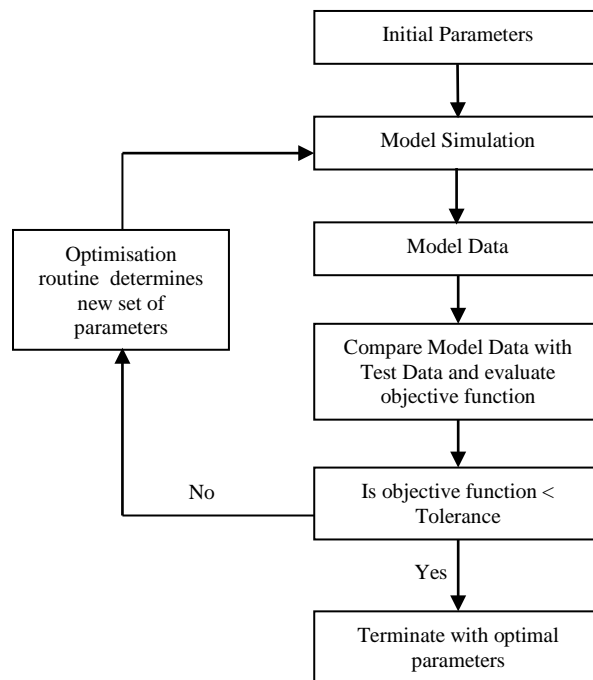
159 and

(9)	$\lambda^* = \frac{\lambda}{\nu}$
-----	-----------------------------------

160 Noting that  $\Lambda$  can also be defined in terms of these composite parameters (i.e.  $\Lambda = (\lambda^* - \kappa^*)/\lambda^*$ ).

161 **OPTIMISATION PROCESS**

162 Optimisation problems require the search for the minimum value of an ‘objective function’, which  
 163 measures the overall difference between numerically generated model data and measured test data. The  
 164 difference between a given set of model and test data is expressed as a single scalar value,  $I$ . A high  
 165 value of the objective function  $I$  indicates a large difference between the model and test data, a value of  
 166 zero indicates a perfect match. The general optimisation process is illustrated in Figure 4.



167

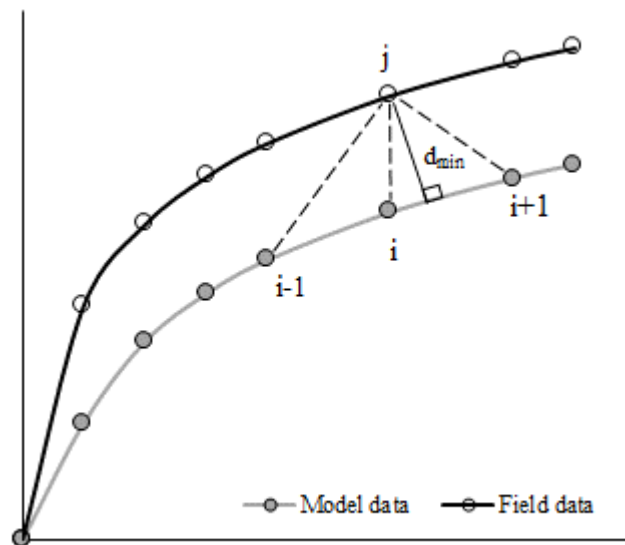
168 Figure 4: Flow chart showing general optimisation process.

169 There are a number of rational methods for comparing model and test data and computing the value of  
 170 the objective function  $I$ . In this study, the objective function was formed by summing the minimum

171 distances of each of the  $n$  test data points from a straight-line fit between the two nearest model data  
 172 points ( $d_{min}$ ) [7], as shown in Figure 5, where

(10)	$I = \frac{1}{n} \left( \sum_{j=1}^n d_{min}^j \right)$
------	---

173



174

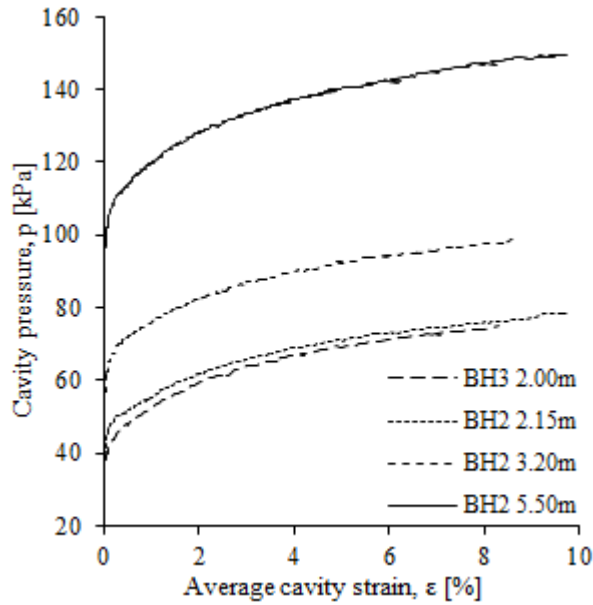
175 Figure 5: Derivation of a scalar value to describe the difference of two curves.

176 The advantages of using this procedure in forming the objective function are discussed in detail by [7].

## 177 TARGETED NUMERICAL OPTIMISATION STRATEGY

### 178 *Overview*

179 The systematic optimisation strategy developed in this study to derive a set of MCC parameters for  
 180 boundary value problems that are dominated by undrained shearing using SBPM test data is described  
 181 in this section. The strategy was applied to eight SBPM test results over a range of depths relevant to  
 182 the shallow foundation problem to which the results are later applied. The tests were selected as they  
 183 did not involve unload-reload loops, or creep holds and were conducted at a strain rate that ensured  
 184 undrained behaviour. Example stress-strain data for four of the selected tests are shown in Figure 6.



185

186 Figure 6: Cavity pressure – cavity strain response for a selection of the SBPM field tests considered in  
 187 this study.

188 Prior to the optimisation stage, the initial mean effective stress,  $p'_i$ , and undrained shear strength,  $s_u$ , for  
 189 each test depth was calculated from well-established methods. The approaches adopted for determining  
 190  $p'_i$  and  $s_u$  for this study are set out below. A sensitivity study is then presented to examine the relative  
 191 influence of each MCC parameter on the computed pressuremeter response in order to reduce the  
 192 parameter space for the subsequent optimisation stage. The optimisation strategy is then presented.

193

194 *Mean effective stress determination*

195 The initial mean effective stress ( $p'_i$ ) at each test depth was calculated by estimating the total vertical  
 196 stress ( $\sigma_v$ ) based on the soil density and the total horizontal stress based on the lift off pressure from the  
 197 SBPM data ( $\sigma_h$ ). Effective stresses were determined by subtracting the in situ static pore pressure ( $u$ ).

(11)	$p'_i = \frac{(\sigma_v + 2\sigma_h)}{3} - u$
------	---

198

199

200 *Undrained shear strength determination*

201 The undrained shear strength ( $s_u$ ) can be estimated from SBPM data using a well-established approach  
 202 ([17], [18]), describing the relationship of cavity pressure ( $p$ ) and volumetric strain ( $\Delta V/V$ ) through

(12)	$p = p_l + s_u \ln\left(\frac{\Delta V}{V}\right)$
------	--

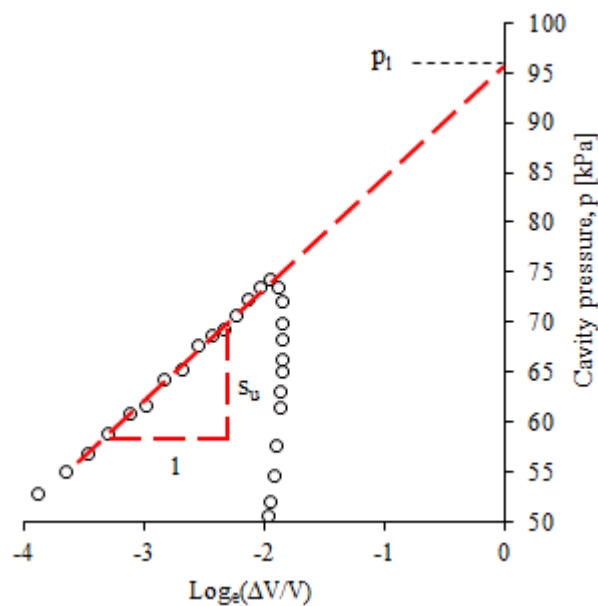
203 where  $p_l$  is the limit pressure,  $\Delta V$  is the cavity volume change and  $V$  is the current cavity volume ( $V_0 +$   
 204  $\Delta V$ ) at the measured pressure. This relationship is only valid for the plastic part of the pressure – strain  
 205 curve when

(13)	$p \geq \sigma_h + s_u$
------	-------------------------

206 where  $\sigma_h$  is the in situ horizontal stress. The limit pressure is a theoretical value that is reached after  
 207 infinite expansion of the pressuremeter and is given by:

(14)	$p_l = \sigma_h + s_u \left( 1 + \ln\left(\frac{G}{s_u}\right) \right)$
------	---

208 The cavity pressure versus cavity strain on a semi-logarithmic plot becomes linear as plastic strain  
 209 governs, with the gradient of the slope being equal to the undrained shear strength  $s_u$ , as shown in Figure  
 210 7.



211  
 212 Figure 7: Example demonstrating the estimation of undrained shear strength  $s_u$  from SBPM data.

213 The mean effective stress and the undrained shear strength for the eight tests considered in this study  
 214 are given in Table 2 along with the borehole reference, depth and loading rate.

215 Table 2: Pressuremeter test details considered in this study.

Borehole	Depth [m]	$s_u$ [kPa]	$p'_i$ [kPa]	Loading rate [kPa/min]
BH 2	2.15	10.5	24.5	10
BH 2	3.20	11.4	31.4	10
BH2	4.15	12.8	45.0	10
BH 2	5.50	15.3	50.0	10
BH 3	2.00	11.0	23.6	25
BH3	3.00	14.6	32.0	50
BH4	3.00	9.4	31.0	1
BH4	4.00	10.0	39.5	1

216

217

218 *Parameter sensitivity analysis*

219 With values for undrained strength and initial mean effective stress,  $s_u$  and  $p'_i$ , established from standard  
 220 interpretation methods (as described above), the MCC formulation for undrained shear strength, given  
 221 in Equation (5), can be used to constrain the possible combination of MCC parameter values  $M$ ,  $A$  and  
 222  $R_0$ . To develop an efficient process for evaluating these parameters, a study was carried out to examine  
 223 the relative influence of these three parameters on the computed pressuremeter stress-strain response.  
 224 The values used in the parametric study were constrained to fall within a typical range for soft clays  
 225 [19].

226 Figure 8a shows the effect on the stress-strain response of varying the ratio  $A$  (between 0.70 and 0.99)  
 227 while the isotropic overconsolidation ratio was fixed to  $R_0 = 1.1$ . The free variable,  $M$ , was evaluated  
 228 by re-arranging Equation (5) (see equation (15)). For the example shown in Figure 8, values of  $s_u = 15.3$   
 229 kPa and  $p'_i = 50$  kPa were adopted to correspond to the test depth of 5.5 m (see Table 2).

(15)

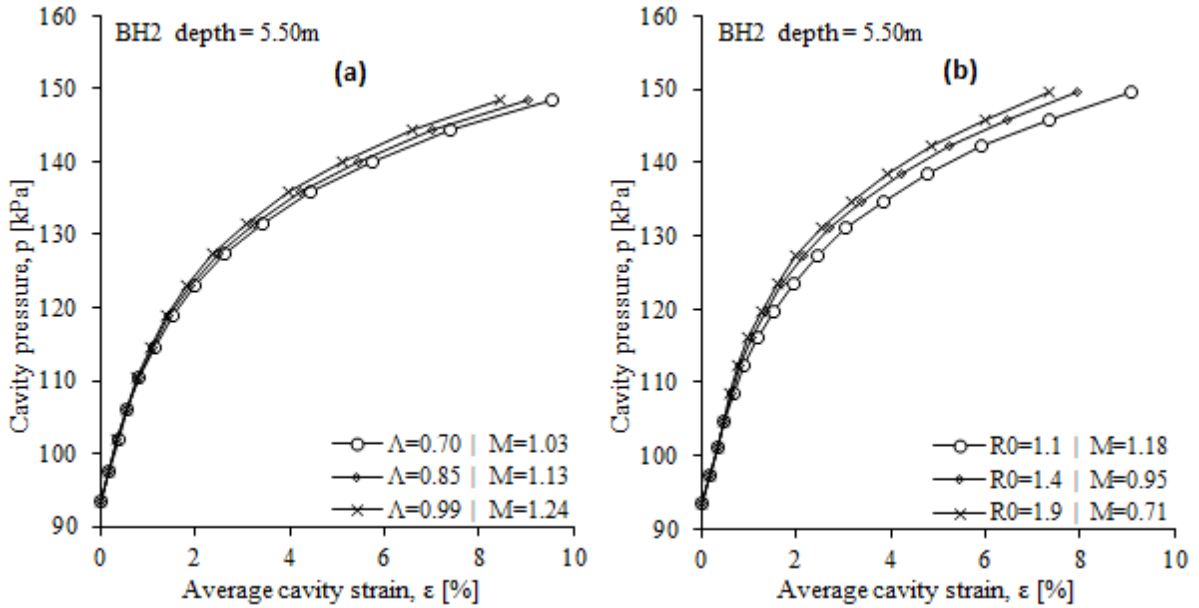
$$M = \frac{2s_u}{p'_i} \left( \frac{R_0}{2} \right)^{-\Lambda}$$

230

231 It can be seen from Figure 8a that for constant values of  $p'_i$ ,  $R_0$ , and  $s_u$ , changes in  $\Lambda$  and  $M$ , over a  
232 relatively large range, have very little impact on the computed undrained stress-strain response.

233 A similar study was conducted by fixing  $\Lambda = 0.8$  and varying  $R_0$  between 1.1 and 1.9, with  $M$  again  
234 evaluated to satisfy  $s_u = 15.3$  kPa and  $p'_i = 50$  kPa for the test at 5.5m. Curves within each figure were  
235 compared by computing  $I$  using Equation (10). It was found that the isotropic overconsolidation ratio  
236  $R_0$  had a more significant impact on the computed undrained pressuremeter response than the other  
237 variables, as the value of  $I$  for the curves in Figure 8b (in which  $R_0$  was varied) was double that of those  
238 in Figure 8a (in which  $\Lambda$  was varied).

239



240

241 Figure 8: Parameter impact on the numerical SBPM stress-strain response  
242 (a) of varying  $M$  and  $\Lambda$  with a fixed value of  $R_0 = 1.1$  and (b) of varying of  $R_0$  and  $M$  with fixed value  
243 of  $\Lambda$ .

244 This indicates that of the three unknown parameters in the MCC formulation for undrained strength,  
245 Equation (5),  $R_0$  has the most significant influence on the stress-strain response. Sensitivity studies

246 conducted on tests at other depths resulted in similar findings. Based on this,  $R_0$  was included in the  
247 optimisation procedure outlined below. Of the two remaining parameters (that have been shown to have  
248 minimal impact on the numerical response),  $\lambda$  typically falls in the narrowest range for soft clays [19].  
249 Therefore, to proceed with the parameter determination process,  $\lambda$  was fixed to a representative value  
250 allowing  $R_0$  to be varied in the parameter selection process while  $M$  is determined from Equation (15).  
251 Linking these three parameters through Equation (15) constrains the search space and ensures that the  
252 resulting parameter set will give the same undrained shear strength as that determined from traditional  
253 interpretation methods [18].

254

255 The remaining MCC parameters,  $\kappa^*$  and  $\mu$  (see Table 1) have no influence on the undrained shear  
256 strength, but significantly impact the stiffness (see Equation (4)). Of these parameters, Poisson's ratio,  
257  $\mu$ , has the narrowest range; typically, 0.1 - 0.4 (a factor of 4) compared with  $\kappa^*$  that could vary by a  
258 factor of 50. On this basis, a strategy that involved a parametric sweep over  $\mu$  and the application of  
259 numerical optimisation to identify  $\kappa^*$  is outlined below.

260

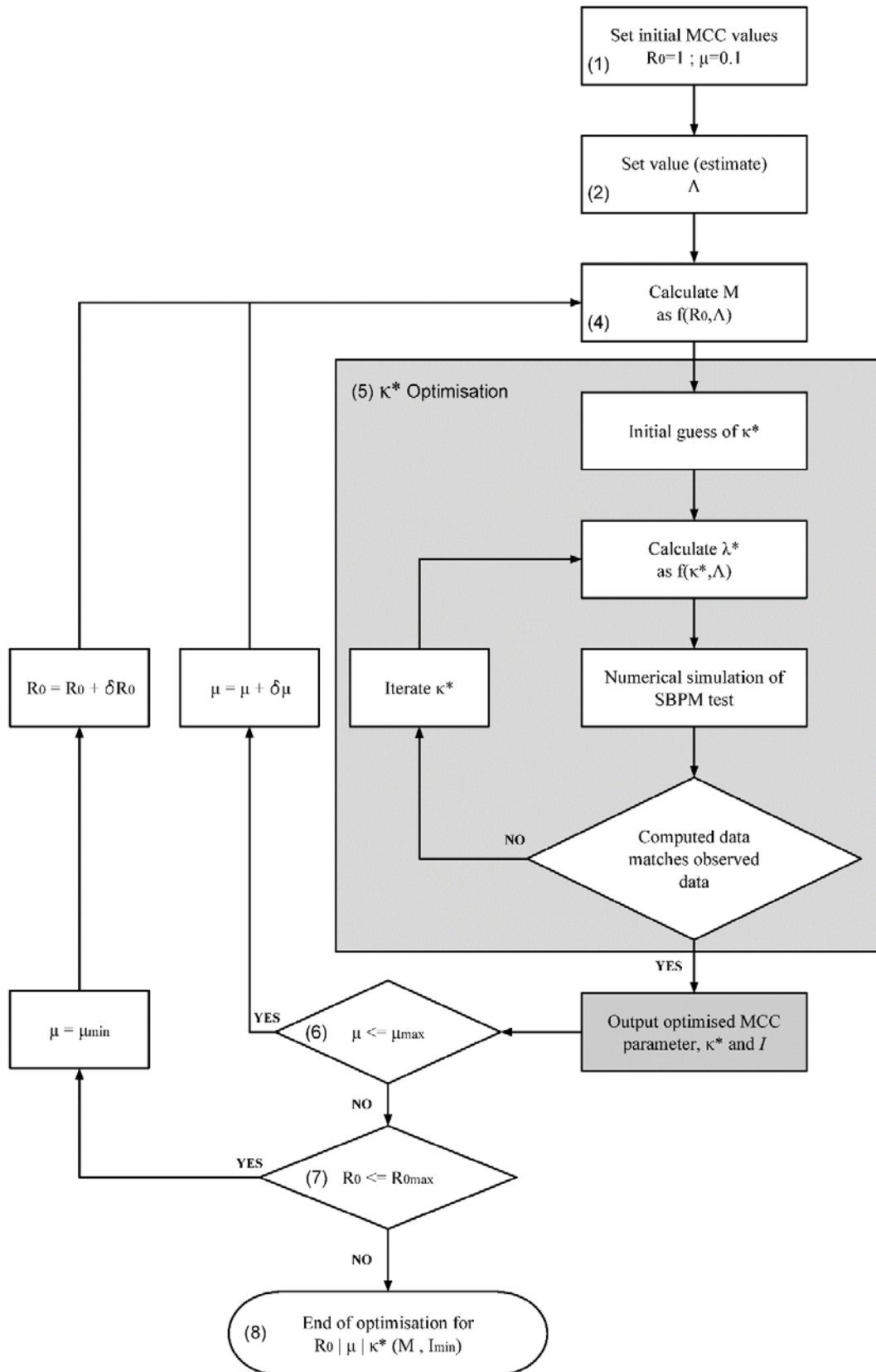
### 261 *Optimisation strategy*

262 The nested single variable optimisation strategy developed in this study is illustrated in Figure 9, and  
263 can be described in the following steps:

- 264 1. Estimate the initial mean effective stress,  $p'_i$ , and the undrained shear strength,  $s_u$ , from SBPM  
265 data (as described above).
- 266 2. Set an initial value (estimate) for the composite parameter  $\lambda$  within an acceptable range.
- 267 3. Set the maximum ( $R_0^{max}$ ,  $\mu^{max}$ ), minimum ( $R_0^{min}$ ,  $\mu^{min}$ ) and incremental values ( $\delta R_0$ ,  $\delta \mu$ ) for  
268 the isotropic over consolidation ratio,  $R_0$  and Poisson's ratio,  $\mu$ . To begin with set  $R_0 = R_0^{min}$   
269 and  $\mu = \mu^{min}$ .
- 270 4. Compute  $M$  from Equation (15) for a given  $p'_i$ ,  $s_u$ ,  $\lambda$  and  $R_0$ .

- 271 5. Conduct single variable optimisation to compute an optimal value of  $\kappa^*$  with  $p'_i, s_u, A, R_0, M$   
272 and  $\mu$  and store the value of the objective function,  $I$ , (Equation (10)) for the optimum value  
273 of  $\kappa^*$ .
- 274 6. If  $\mu < \mu^{max}$  increase  $\mu$  by  $\delta\mu$  and go to step 5, otherwise go to step 7.
- 275 7. If  $R_0 < R_0^{max}$  increase  $R_0$  by  $\delta R_0$  and go to step 4, otherwise go to step 8
- 276 8. The outcome is a table of parameters ( $A, R_0, M$  and  $\mu$  and  $\kappa^*$ ) along with the value of the  
277 objective function ( $I$ ) for each parameter set.
- 278 9. Select the set of parameters with the lowest value of  $I$ .





279

280 Figure 9: Nested single variable optimisation strategy to derive MCC parameters from SBPM test data

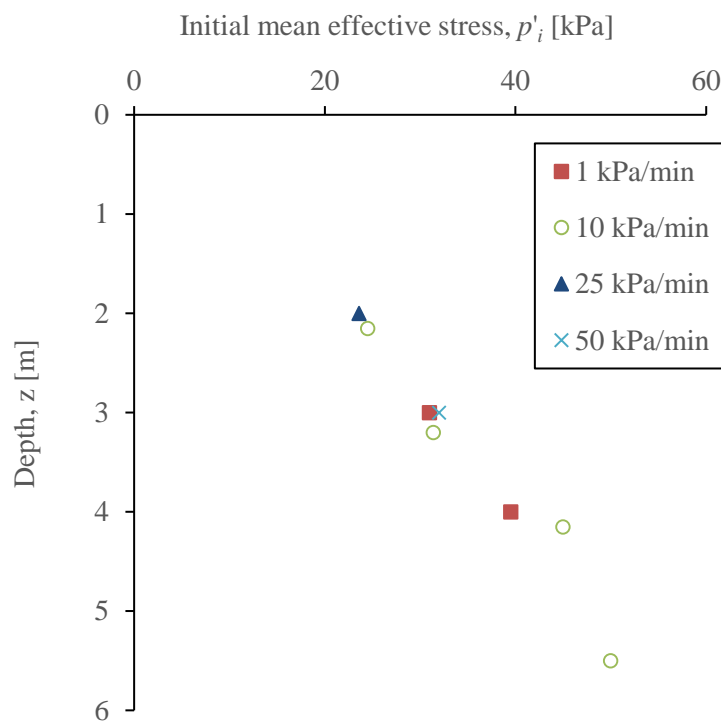
281

developed in this study.

282 **RESULTS**

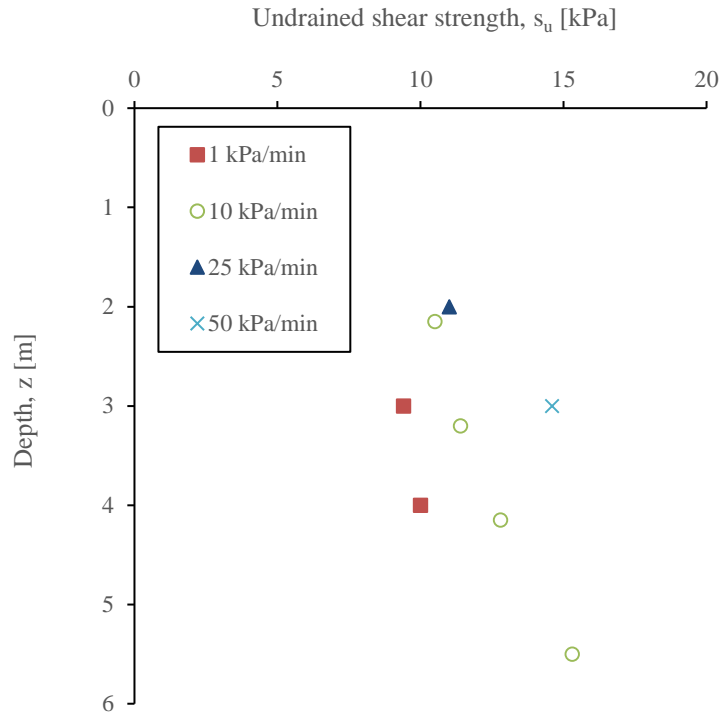
283 The optimisation strategy described above and summarised in Figure 9, was applied to derive MCC  
284 parameters for the eight SBPM tests listed in Table 2.

285 The mean effective stress,  $p'$ , is plotted against depth in Figure 10 for all eight tests. The undrained  
286 shear strength,  $s_u$  is plotted in Figure 11. The loading rate of the test, i.e. the rate of pressure increase  
287 during the SBPM test, is noted in the figures. It can be seen from Figure 11 that higher loading rates  
288 result in higher undrained shear strengths, which may be an indication of viscous effects. The following  
289 values were set for the parametric sweep;  $R_0^{min} = 1$ ,  $R_0^{max} = 2$ ,  $\delta R_0 = 0.1$ ,  $\mu^{min} = 0.1$ ,  $\mu^{max} = 0.4$  and  $\delta\mu =$   
290  $0.1$ . Once the optimal value for  $R_0$  was identified using these search parameters, a second sweep was  
291 conducted in a narrow range of 0.1 either side of the optimal value of  $R_0$  using  $\delta R_0 = 0.02$ .



292

293 Figure 10: Initial mean effective stress profile from the eight SBPM tests considered in this study.



294

295 Figure 11: Undrained shear strength profile from the eight SBPM tests considered in this study.

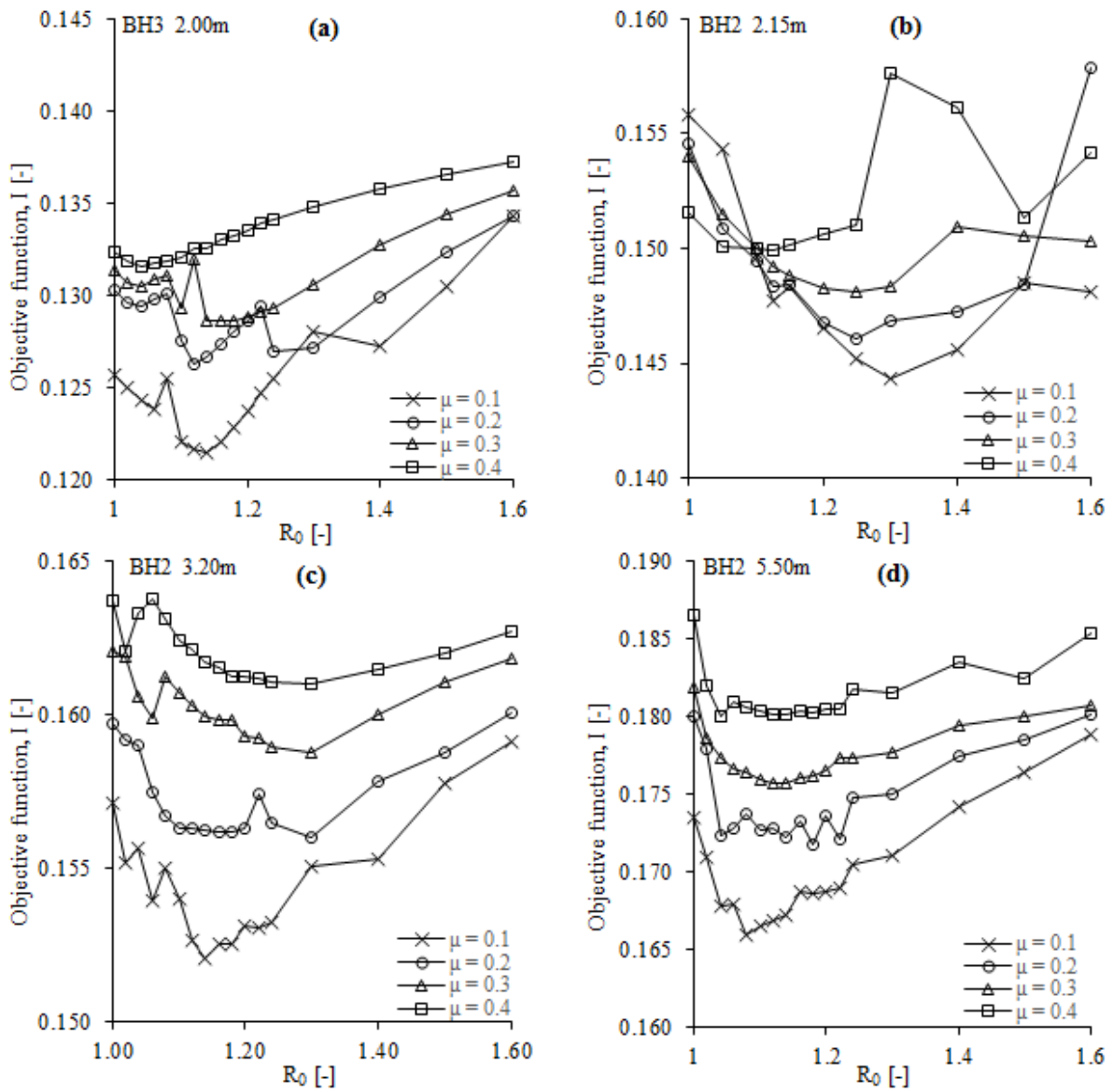
296 Figure 12 plots the results from the shaded box in Figure 9, i.e. the minimum value of the objective  
 297 function,  $I$ , for each combination of  $R_0$  and  $\mu$  for optimised values of  $\kappa^*$  for four selected tests. Similar  
 298 results were observed for the other four tests, but are not presented due to space restrictions. For each  
 299 point in Figure 12,  $\kappa^*$  was evaluated using the optimisation function *fminbd* in MATLAB. The function  
 300 *fminbd* is based on the golden search section method and uses parabolic interpolation to find the  
 301 minimum to a nonlinear function of a single bounded variable (MathWorks® 2010). During the  
 302 optimisation process lower and upper bounds of  $\kappa^*$  were specified as 0.001 and 0.05.

303 Figure 13 plots the value of the objective function ( $I$ ) against the value of the composite unload-reload  
 304 compression index  $\kappa^*$  sampled by *fminbd* throughout the optimisation process for the full range of  
 305 Poisson's ratio  $\mu$  values with a single value of isotropic overconsolidation ratio  $R_0 = 1.08$  for a single  
 306 SBPM test at a depth of 5.50 m. It can be seen that a very clear minimum exists for each value of  $\mu$  and  
 307 therefore *fminbd* converges rapidly to the optimal value of  $\kappa^*$  (with other parameters fixed) in around  
 308 10 function evaluations. For each SBPM test, four values of  $\mu$  and ten values of  $R_0$  were trialled and  $\kappa^*$   
 309 convergence typically required around 10 function evaluations. The total number of function

310 evaluations for each test is therefore  $10 \times 4 \times 10 = 400$ . It can be seen from Figure 12 that the smallest  
311 value of  $\mu$  (i.e.  $\mu^{min}$ ) results in the optimal or near optimal match to the data (i.e. smallest value of  $D$ ).  
312 This is consistent with a previous study that showed  $\mu$  tended towards the minimum allowable value  
313 when matching MCC parameters to undrained triaxial compression data [11]. It is therefore possible  
314 that  $\mu$  could be removed from the parametric sweep and the lowest acceptable value of  $\mu$  adopted. This  
315 would reduce the parametric sweep to around 100 function evaluations. The optimised parameters for  
316 each test are listed in Table 3.

317 Table 3: Optimised MCC parameters

Borehole	Depth [m]	Loading rate (kPa/min)	M [-]	$\Lambda$ [-]	$\mu$ [-]	$\kappa^*$ [-]	$R_0$ [-]
BH 2	2.15	10	1.276	0.92	0.1	0.0241	1.3
BH 2	3.20	10	1.22	0.92	0.1	0.0228	1.14
BH 2	4.15	10	0.91	0.92	0.1	0.0299	1.2
BH 2	5.50	10	1.2	0.92	0.1	0.0261	1.08
BH 3	2.00	25	1.56	0.92	0.1	0.0221	1.14
BH 3	3.00	50	1.65	0.92	0.1	0.0306	1.04
BH 4	3.00	1	0.99	0.92	0.1	0.0321	1.16
BH 4	4.00	1	0.76	0.92	0.1	0.0294	1.28

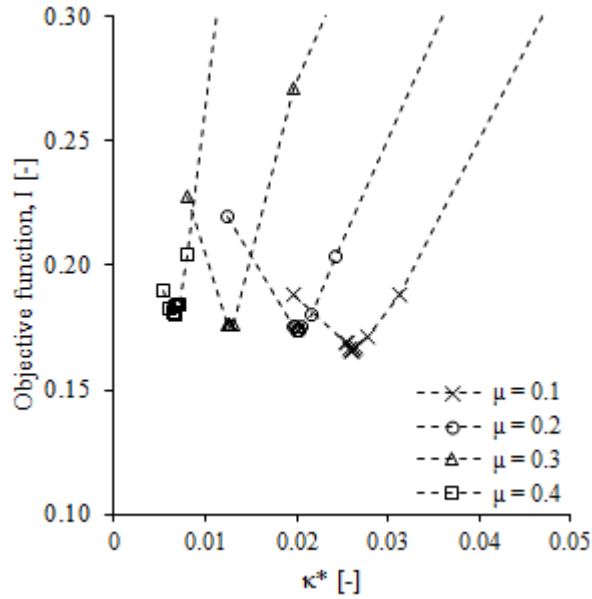


319

320 Figure 12: Objective function  $I$  for a range of  $\mu$  and  $R_0$  values for selected tests; a) test BH3 2.00m; b)

321

test BH2 2.15m; c) test BH 3.20m and d) test BH2 5.50m.



322

323

Figure 13: Optimisation of  $\kappa^*$  for a range of  $\mu$  values for  $R_0 = 1.08$  (Test BH2 5.50m).

324

The stress-strain responses using the optimised MCC parameters are compared to four of the field tests

325

in Figure 14. It can be seen that the MCC model generally gives a good match to the field data, although

326

slightly under predicts the stiffness at lower strain levels. It is noted that as a fully coupled model is

327

used in an undrained loading regime, volumetric strains are prevented by including the bulk stiffness of

328

the pore fluid. The primary influence of Poisson's ratio is on the initial shear stiffness and the value of

329

the initial shear stiffness increases as Poisson's ratio decreases (see Equation (4)). The fact that optimal

330

value of  $\mu$  was the lowest allowable value in each test indicates that the match to the data at low strain

331

levels is limited by the constraint on Poisson's ratio. Theoretically, Poisson's ratio may range between

332

0.5 (infinite volumetric stiffness) and  $-1$  (infinite shear stiffness). However, very low or negative

333

Poisson's ratio will result in low or negative ratios of the change in horizontal and vertical effective

334

stress in one-dimensional unloading or reloading. This is likely to be unacceptable in general

335

applications of the model. It was therefore considered reasonable to limit the minimum value of

336

Poisson's ratio to 0.1. Very similar conclusions were drawn when fitting MCC parameters to triaxial

337

compression data [11]. This highlights a limitation of the MCC model. How significant this limitation

338

is when it comes to using the model to make field prediction is assessed in the following section of this

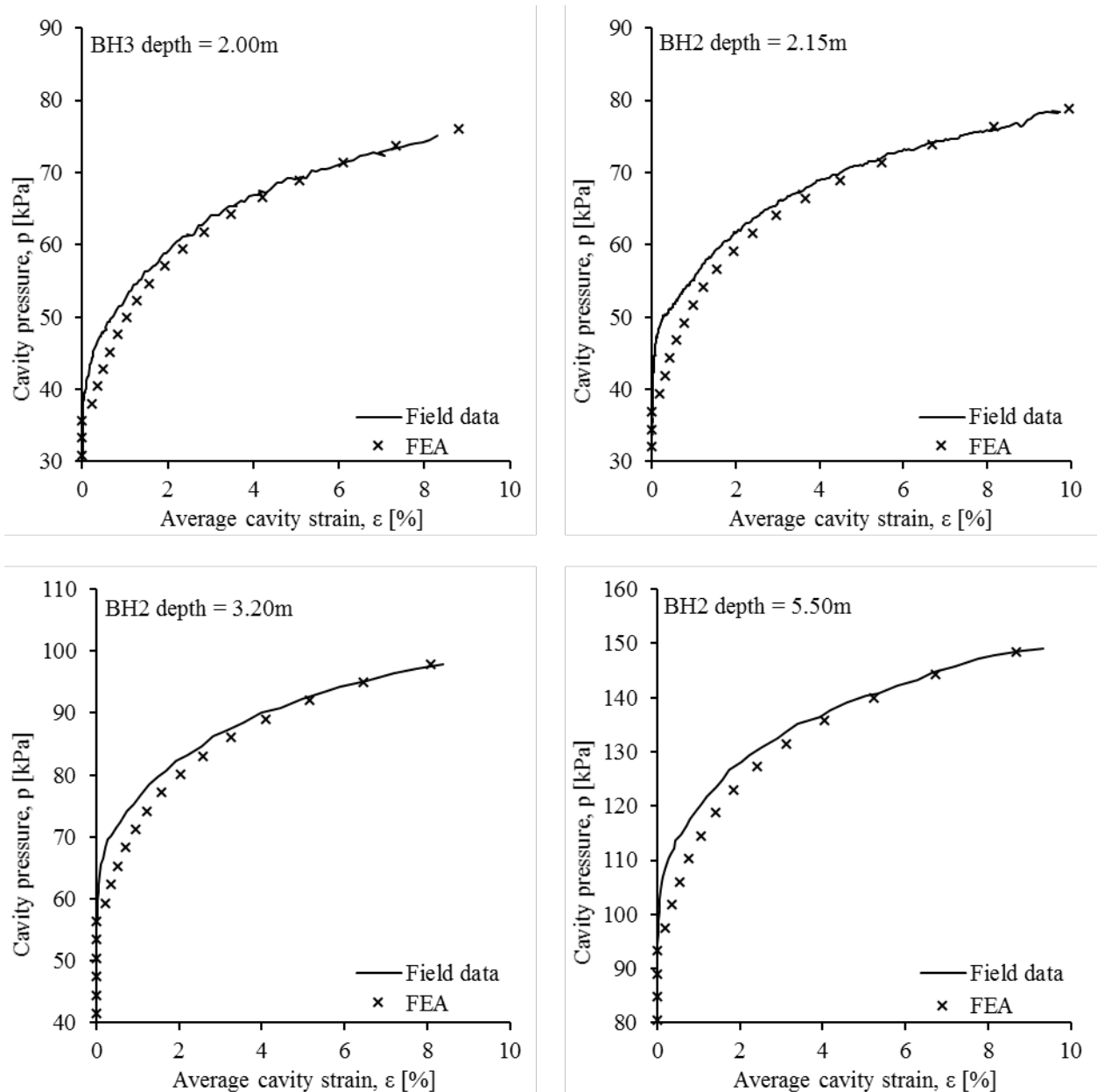
339 paper by using the optimised parameters to back analyse the response of two shallow foundations  
340 subject to undrained vertical loading.

341

342

343

344



345

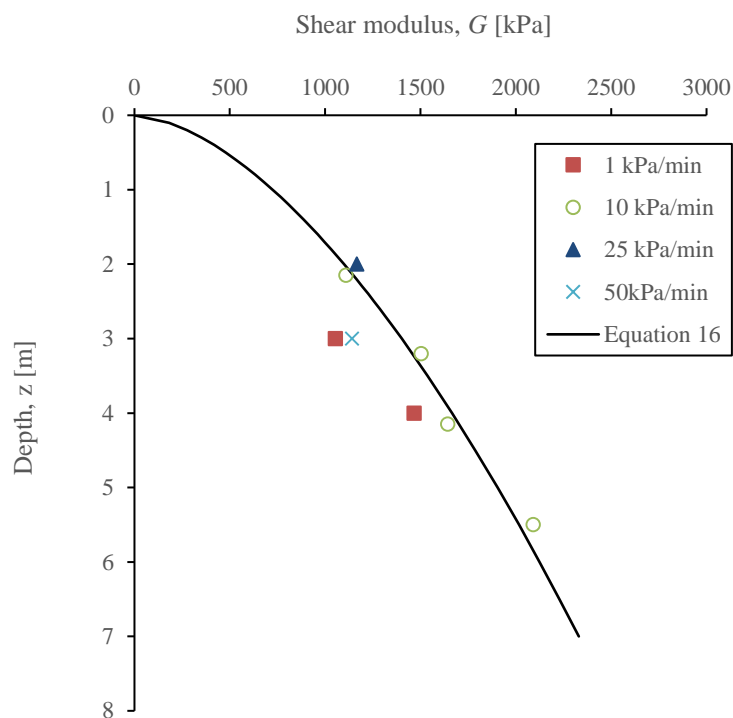
346

347 Figure 14: Examples of observed stress–strain response from SBPM tests compared with computed  
348 response using the optimised MCC parameter set.

349 Figure 15 plots the shear modulus against depth, as defined by Equation (4) and the parameter values  
 350 in Table 3. Based on [20] the variation of shear modulus ( $G$ ) with depth  $z$  was fitted using the following  
 351 equation

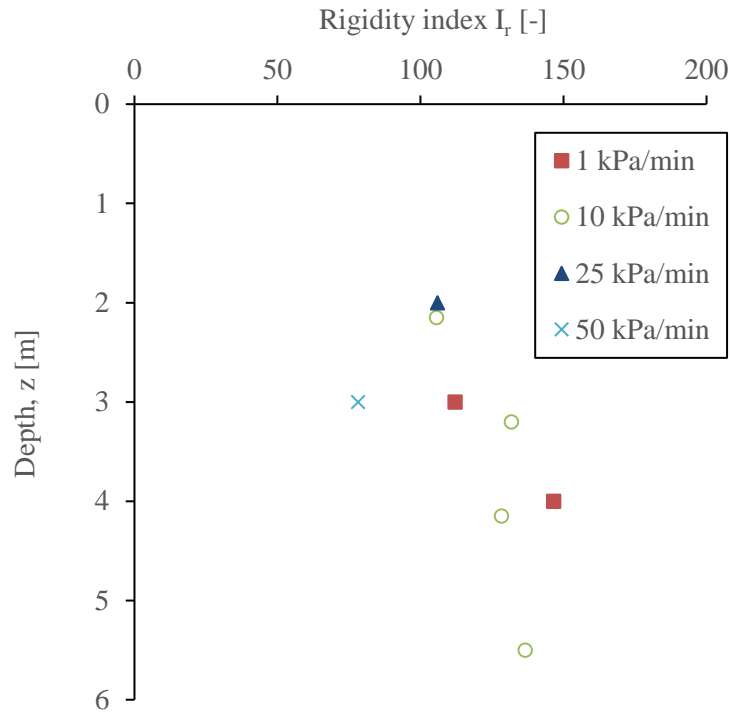
(16)	$G = G_1 \cdot z^\alpha$
------	--------------------------

352  
 353 where the exponent  $\alpha = 0.6$  and  $G_1 = 725$  (kPa) is the shear modulus at  $z = 1$  m. This form of power  
 354 law variation is considered reasonable for normally consolidated sand and soft clay [21]. The rigidity  
 355 index ( $G/s_u$ ) is plotted against depth in Figure 16. Except for the pressuremeter tests with the higher  
 356 loading rate of 50 kPa/min, the rigidity index values are consistent with results from other studies at the  
 357 NFTF in Ballina [22].



358  
 359 Figure 15: Shear modulus with depth calculated with optimised  $\kappa^*$ .





360

361

Figure 16: Rigidity index with depth predicted with optimised MCC parameter set.

362

## VALIDATION

363

As shown in Figure 1, two large scale foundation load tests were carried out at the NFTF within 30 m of the pressuremeter tests that have been presented in this paper. Data from these foundation load tests provide an ideal opportunity to validate the parameter selection procedure described in this paper. The tests involved two 1.8 m square concrete foundations cast in an excavation 1.5 m below ground surface.

367

The foundations were loaded undrained to failure while foundation displacements were recorded through surveying targets. A detailed description of the field testing is reported in the literature [23].

369

The numerical simulation of the shallow foundation was carried out with the Abaqus finite element software package. An axisymmetric finite element model was created with the radius of the circular foundation set to give the same area as the actual square foundations and the area of the gap between the edge of the foundation and the edge of the excavation also set equivalent to the field conditions (Figure 17). Using an axisymmetric model to idealise a square foundation in this way has been shown to have minimal effect on the bearing capacity of a shallow foundation under uniaxial vertical load [24] (Gourvenec et al. 2006). The axisymmetric model was selected as a pragmatic approach, and one more

373

374

375

376 likely to be adopted in engineering practice than a full 3D analysis. The mesh comprised using 4840  
 377 quadratic elements, determined through a sensitivity analysis to ensure sufficient mesh refinement was  
 378 achieved. The base and circumferential boundaries were positioned sufficiently remote from the  
 379 foundation so as not to influence the results.

380

381 The upper 1.5 m thick clayey silty sand was modelled as an elastic perfectly plastic material and the  
 382 estuarine clay was modelled with in-built MCC material model (Clay plasticity) using four different  
 383 layers. The parameters for the MCC model used in the analysis are presented in Table 4. These  
 384 parameters are based on a pressuremeter loading rate of 10 kPa/min. The loading rate of 10kPa/min was  
 385 chosen as data at this rate is available from a single borehole throughout the depth of the soft soil profile  
 386 and therefore provides the most consistent set of parameters. This provides an opportunity to determine  
 387 if 10kPa/min is a suitable loading rate to predict the response of a shallow footing loaded to failure over  
 388 a time period of approximately 1 hour..

389 Table 4: Optimised parameter set for MCC model used in foundation model

Depth [m]	M [-]	R <sub>0</sub> [-]	κ* [-]	Λ [-]	μ [-]
1.5 – 2.0	1.33	1.28	0.023	0.92	0.1
2.0 – 3.0	1.26	1.21			
3.0 – 5.0	1.22	1.12			
5.0 - 10	1.20	1.08			

390

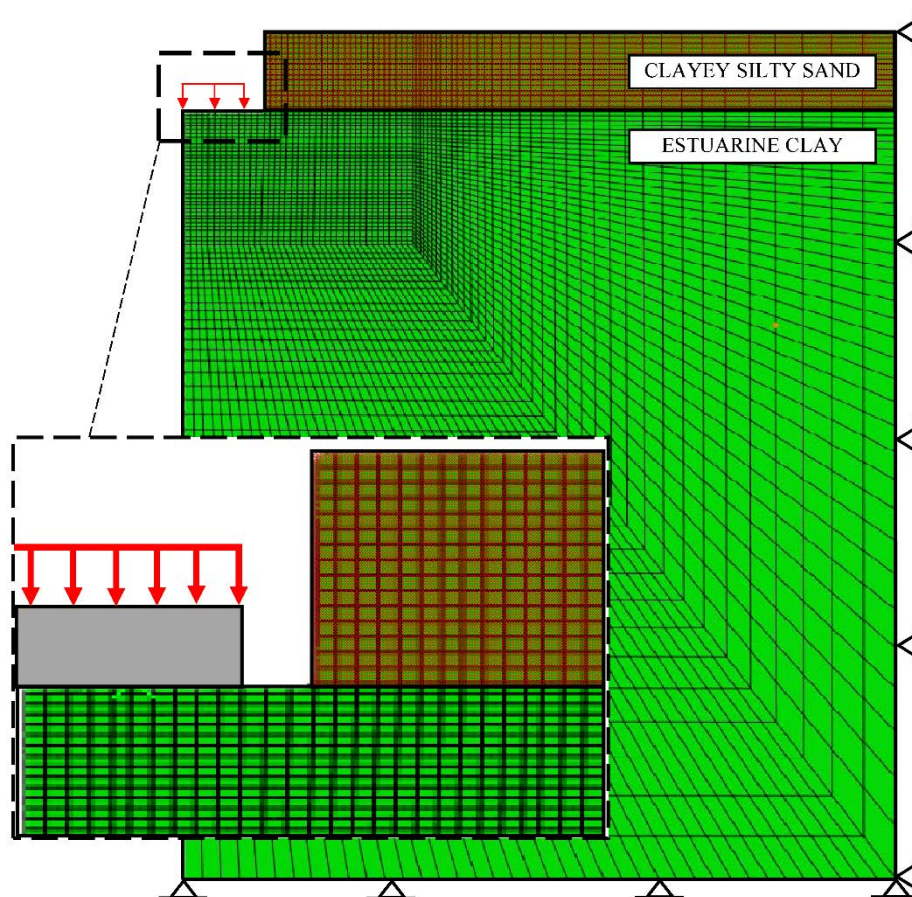
391 The simulation of the foundation tests comprised four major analysis steps:

- 392 1. Excavation of the foundation pit (unloading of the estuarine clay)
- 393 2. Construction of the foundation (reloading)
- 394 3. Consolidation period
- 395 4. Final undrained loading to failure

396 Observed and predicted load-settlement response to failure are shown in Figure 18. The excellent  
 397 agreement between the measured and computed response demonstrates that the optimisation strategy

398 set out in this paper for evaluating MCC parameters from SBPM data provides a practical and efficient  
399 approach to extrapolate SBPM data to predict the response of more complex undrained boundary value  
400 problems.

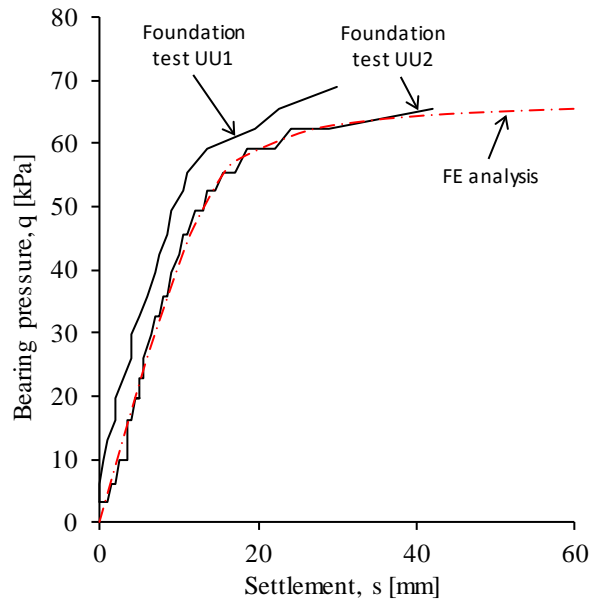
401 A significant attribute of the procedure presented in this paper is that, once the vertical effective stress  
402 and pore pressure at the test location have been determined, the remainder of the parameter selection  
403 process is entirely automated. This means that there is less subjectivity and use of engineering  
404 judgement. The foundation data presented in Figure 18 was the subject of an international prediction  
405 exercise, where 50 groups of engineers on average over predicted the capacity of the foundation by  
406 100% and the settlement at working loads by more than 1000%. The primary reason for the poor  
407 predictions was attributed to the way in which engineers interpret geotechnical test data. Automated  
408 interpretation techniques, such as the one set out in the paper, are therefore critical in improving  
409 predictive performance.



410

411

Figure 17: FE model of large scale foundation tests at the NFTF.



412

413 Figure 18: Observed and computed load-settlement response of shallow foundation tests conducted at  
 414 the NFTF in Ballina, NSW.

415 **CONCLUSIONS**

416 A new, efficient, practical and automated strategy has been presented for deriving an optimised set of  
 417 Modified Cam Clay parameters from undrained self-boring pressuremeter test data using a strategic  
 418 combination of traditional interpretation methods, a parametric sweep and numerical optimisation  
 419 techniques.

420 The method was derived by examining the Modified Cam Clay formulation to identify groups of  
 421 parameters that control various features of undrained cavity expansion. Established methods are used  
 422 to derive the initial mean effective stress and undrained shear strength, based on data from the start and  
 423 finish of the cavity pressure-cavity strain curve, respectively. This information is then used to constrain  
 424 the parameters that link effective stress and undrained shear strength. This limits the possible set of  
 425 valid soil parameters and reduces the parameter search space allowing an efficient technique, combining  
 426 a parametric sweep with a single variable optimisation, to automatically select the optimal, or near  
 427 optimal, values for the remaining soil parameters. This approach has been developed into a powerful  
 428 and versatile tool that automates parameter selection from pressuremeter data. The resulting parameters  
 429 were found to depend on the rate of pressuremeter loading. Parameters derived from a pressuremeter

430 loading rate of 10kPa/min were found to provide an excellent back analysis of the undrained load-  
431 settlement response of a 1.8m square shallow foundation loaded to failure in approximately 1 hour.  
432 Even though the process described is automated and removes subjectivity, it is fully auditable and  
433 engineers can use their expertise to critically assess the validity of the parameters that are derived

#### 434 **ACKNOWLEDGEMENTS**

435 This work forms part of the activities of the Centre for Offshore Foundation Systems (COFS).  
436 Established in 1997 under the Australian Research Council's Special Research Centres Program.  
437 Supported as a node of the Australian Research Council's Centre of Excellence for Geotechnical  
438 Science and Engineering. This support is gratefully acknowledged.

#### 439 **REFERENCES**

- 440 [1] Doherty JP, Gaone FM, Gourvenec S. Insights from a shallow foundation load-settlement  
441 prediction exercise. *Comput Geotech* 2017. doi:[http://dx.doi.org/  
442 10.1016/j.compge.2017.05.009](http://dx.doi.org/10.1016/j.compge.2017.05.009).
- 443 [2] Lehane BM. Vertically loaded shallow foundation on soft clayey silt. *Proc Inst Civ Eng -  
444 Geotech Eng* 2003;156:17–26. doi:10.1680/geng.2003.156.1.17.
- 445 [3] Lehane B, Doherty JP, Schneider JA. Settlement prediction for footings on sand. 4th Int. Symp.  
446 Deform. Charact. Geomaterials, Atlanta: IOS press, The Netherlands; 2008, p. 133–50.
- 447 [4] Briaud J-L, Gibbens R. Large scale load tests and database of spread footings on sand. *Fed  
448 Highw Adm Rep No FHWA-RD-97 1997*.
- 449 [5] Klisinski M. Optimisation program for identification of constitutive parameters. *Struct Res Ser  
450 1987*.
- 451 [6] Wood DM, Mackenzie NL, Chan AHC. Selection of parameters for numerical predictions.  
452 *Predict Soil Mech Proc Wroth Meml Symp Oxford, 1992 1992:496–512*.
- 453 [7] Mattsson H, Klisinski M, Axelsson K. Optimization routine for identification of model  
454 parameters in soil plasticity. *Int J Numer Anal Methods Geomech* 2001;25:435–72.  
455 doi:10.1002/nag.137.

- 456 [8] Navarro V, Candel M, Barenca A, Yustres A, García B. Optimisation procedure for choosing  
457 Cam clay parameters. *Comput Geotech* 2007;34:524–31. doi:10.1016/j.compgeo.2007.01.007.
- 458 [9] Calvello M, Finno RJ. Selecting parameters to optimize in model calibration by inverse analysis.  
459 *Comput Geotech* 2004;31:411–25. doi:10.1016/j.compgeo.2004.03.004.
- 460 [10] Taborda D, Pedro A, Coelho P. Impact of input data on soil model calibration using Genetic  
461 Algorithms. *Numer Methods Geotech Eng - Benz Nord* 2010:69–74.
- 462 [11] Doherty JP, Alguire H, Muir Wood D. Evaluating modified Cam clay parameters from  
463 undrained triaxial compression data using targeted optimization. *Can Geotech J* 2012;49:1285–  
464 92.
- 465 [12] Doherty JP, Gourvenec S, Gaone FM, Kelly RB, Pineda JA, O’Loughlin C, Cassidy MJ, Sloan  
466 SW. A novel web based application for storing, managing and sharing geotechnical data,  
467 illustrated using the National soft soil field testing facility in Ballina, Australia. *Comput Geotech*  
468 2017, 10.1016/j.compgeo.2017.05.007.
- 469 [13] Kelly RB, O’Loughlin CD, Bates L, Gourvenec S, Colreavy C, White DJ, et al. In situ testing at  
470 the National Soft Soil Field Testing Facility, Ballina, New South Wales. *Aust Geomech*  
471 2014;50(4):13–26.
- 472 [14] Gaone FM, Doherty JP, Gourvenec S. Self-boring pressuremeter tests at the National Field  
473 Testing Facility, Ballina NSW. 5th Int. Conf. Geotech. Geophys. Site Characterisation, Gold  
474 Coast, Australia: 2016, p. 761–5.
- 475 [15] Systemes D. ABAQUS 6.14 User guide 2014.
- 476 [16] Roscoe KH, Burland JB. On the generalized stress-strain behaviour of wet clay 1968.
- 477 [17] Gibson R., Anderson WF. In situ measurement of soil properties with the pressuremeter. *Civ*  
478 *Eng Public Work Rev* 1961;56:615–8.
- 479 [18] Windle D, Wroth CP. The use of a self-boring pressuremeter to determine the undrained  
480 properties of clays. *Gr Eng* 1977;10:37–46.
- 481 [19] Wood DM. Soil behaviour and critical state soil mechanics. 1991.  
482 doi:<https://doi.org/10.1017/CBO9781139878272>.
- 483 [20] Doherty JP, Deeks AJ. Scaled boundary finite-element analysis of a non-homogeneous

- 484 axisymmetric domain subjected to general loading. *Int J Numer Anal Methods Geomech*  
485 2003;27:813–35. doi:10.1002/nag.300.
- 486 [21] Hardin BO, Drnevich VP. Shear modulus and damping in soils: design equations and curves. *J*  
487 *Soil Mech Found Div ASCE* 1972;98:667–92.
- 488 [22] Pineda JA, Suwal LP, Kelly RB, Bates L, Sloan SW. Characterisation of Ballina clay.  
489 *Géotechnique* 2016;66:556–77. doi:10.1680/jgeot.15.P.181.
- 490 [23] Gaone FM, Gourvenec S, Doherty JP. Large scale shallow foundation load tests on soft clay -  
491 at the National Field Testing Facility (NFTF), Ballina, NSW, Australia. *Comput Geotech* 2017.  
492 doi:[http://dx.doi.org/ 10.1016/j.compge.2017.05.008](http://dx.doi.org/10.1016/j.compge.2017.05.008).
- 493 [24] Gourvenec S, Randolph MF, Kingsnorth O. Undrained bearing capacity of square and  
494 rectangular footings. *Intern Journal of Geomech* 2006. May/June, 6(3): 147–157.  
495 [http://dx.doi.org/10.1061/\(ASCE\)1532-3641\(2006\)6:3\(147\)](http://dx.doi.org/10.1061/(ASCE)1532-3641(2006)6:3(147))  
496